

EDAX FOCUS

Optimizing EDS for TEM

Inside This Issue

Page 2
Optimizing EDS for TEM

Page 3
Multifield Mapping

Page 4
EBSD Characterization of Stress Corrosion Cracks in 2124 Aluminum Alloys

Page 6
Training and Events

Page 7
Employee Spotlight

Page 8
Customer News

Transmission Electron Microscopy (TEM) and Scanning TEM (STEM) has been the most effective method to analyze the structure and composition of nanoscale materials. This technique is becoming more popular and widely used with continuous advances in nanotechnology. Analytical TEM/STEMs are integrated with a variety of detectors to obtain information from samples. The most commonly used detectors in TEM are bright field and dark field imaging, electron diffraction, electron energy loss spectroscopy (EELS), and energy dispersive spectroscopy (EDS). Among these detectors, the EDS has unique advantages over other techniques due to their sensitivity in analyzing heavy elements and their ability to acquire a range of elements between Be to U simultaneously. However, the use of multiple detectors in a confined space around the sample creates many challenges for TEM analysis.

The challenge for EDS is finding the most efficient detector configuration for TEM/STEM microscopes. The high spatial resolution inherent in the TEM applications results in a small excitation volume. The small excitation volume in thin samples analyzed in the microscopes does not generate high numbers of X-rays. As a result, there are only a small number of generated X-rays available for EDS detectors. The solution is to configure the EDS detector with the best collection efficiency possible for the intended microscopes.

To optimize collection efficiency, a careful study of solid angle and other factors influencing the performance is required. The detector design with respect to the pole piece and port configuration determine the solid angle, but there are other factors such as collimator design and shadowing of the window silicon grid support that influence the overall collection efficiency.

The solid angle, Ω , is calculated using the formula A/DTS^2 , where A is the effective detector area and DTS is the detector to sample distance. The solid angle of a hemisphere above the sample would be 2π steradians. For an EDS detector, the proportion of the detector area capturing the X-rays within the hemisphere above the sample must be increased.

Therefore, it is easy to assume that a large area detector is desirable in capturing more X-rays. If there were no space limitations and design restrictions, then the assumption would be true. As often is the case, the real application is more complicated and the sensitivity of each variable in solid angle calculations must be understood.

A large area detector does not necessarily give the largest solid angle or the most desirable geometry with respect to the sample. The collection efficiency is most sensitive to the distance between the detector and the sample.

If DTS is reduced by 30% then,

$$\Omega = \frac{A}{(0.70 * DTS)^2} = 2.04 * \frac{A}{DTS^2} \Rightarrow$$

The solid angle is improved by approximately 100%.

If A is doubled in size then,

$$\Omega = \frac{2 * A}{DTS^2}$$

The solid angle is improved by 100%.

If A is doubled in size but DTS is increased by 42% then,

$$\Omega = \frac{2 * A}{(1.42 * DTS)^2} = \frac{A}{DTS^2}$$

The solid angle is not improved at all.

A 30mm² detector at a distance of 12mm has the same solid angle as a 50mm² detector at a distance of 15.5mm. As shown in the example, the DTS has a much bigger impact on improving the solid angle than the detector size. For larger detectors, the challenge in TEM microscopes is the limited space around the pole piece region. The pole pieces are not always simple cone shapes as they are in SEM's. Usually, they are a combination of two cones with different slope angles. Also, the tube housing of the detector can only approach the cone shape to within a few hundred microns. The tube housing cannot make electrical contact with the cone because it would create a ground loop. These limitations make it difficult for detectors to get as close as possible to the sample. Therefore, finding the right combination of detector size and DTS is critical for improving the solid angle. (Cont'd on Pg. 2)

Optimizing EDS for TEM (Cont'd. from Pg. 1)

Depending on the design of microscope, the collimator design plays a major role for optimizing the collection efficiency. The collimators are designed to block many spurious X-rays that can reach the detector (e.g. background X-rays excited by BSEs) and X-rays emanating from the sample outside of the analysis region. If not done properly, the collimation can significantly impact the overall collection efficiency. If the collimator blocks a part of the detector's active area, then the collection solid angle will be reduced. In addition, the EDS detector needs to be installed where it can view the X-rays from above the sample. Any part of the EDS detector below the surface of the sample will lose its collection efficiency. The take-off-angle (TOA), which describes the angle between the sample surface and the center of the detector, must be high enough to avoid any part of the detector being below the sample surface. A lower TOA increases X-ray escape path from the sample, resulting in increased absorption of X-rays and decreased peak-to-background. Therefore, the collimator needs to be designed for the proper detector size, DTS, TOA and microscope to minimize any loss of collection efficiency.



Additional loss of collection efficiency occurs with the ultra thin polymer windows used in the EDS detectors. The ultra thin polymer windows provide high X-ray transmission of low

Figure 1. Ray diagram rendering of the silicon grid support and detector.

energies and mechanical support to withstand differential pressure. For mechanical strength, a rigid silicon grid with open area supports the window. Nominally, the transmission through the grid is 70 to 80%. The thickness of this rigid silicon grid is 380 microns for a 30mm² detector and 760 microns for an 80mm² detector. The thicker silicon grid is required for large area detectors to withstand additional increase in force with larger area. The problem with a thicker silicon grid is the loss of transmission due to the window grid shadowing. A ray diagram rendering software was used to estimate the transmission through the window grid with different thicknesses. Figure 1 shows the model used to estimate the transmission by using a point light source. The transmission is estimated by calculating the proportion of the area on the detector that is illuminated.

The thick silicon grid absorbs the X-rays if they are not transmitted through the open area. Therefore, the ray diagram rendering software provides a very accurate estimate of X-ray transmission through the silicon grid.

Figure 2 and 3 show the transmission comparison between the 30mm² and 80mm² detectors. The 80mm² detector with a thicker support grid has an overall lower transmission compared to a 30mm² detector, which needs to be accounted for in the solid angle modeling.

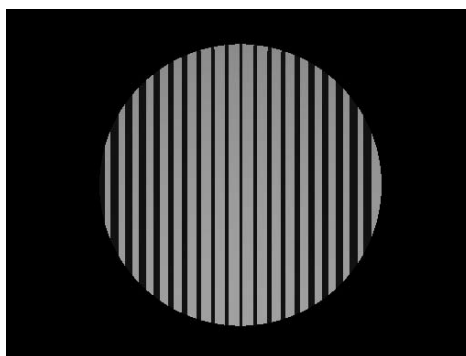


Figure 2. 30mm² detector results with 70% transmission

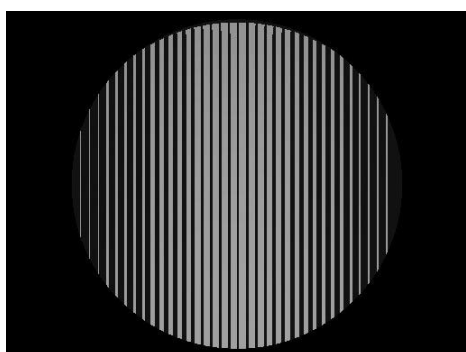


Figure 3. 80mm² detector results with 60% transmission

Collection efficiency improvement is dependent on more than just increasing the crystal size in EDS detectors. The right approach is to optimize the solid angle for intended microscopes ideally considering the various space limitations and design requirements. The TOA and collimator design must be evaluated carefully to minimize any loss of collection efficiency. Any part of the detector that is blocked, decreases collection efficiency. The detector's active area should have a clear view of the sample in the analysis. Even with the clear view, the window grid shadowing further reduces the transmission. Given these variables that impact the collection efficiency, finding the right balance best suited for each microscope is the challenge for the EDS detector manufacturer. EDAX has a long history of working with EMMs to provide the best solution to enhance the capability of the overall system performance. Our experience in the microanalysis industry in combination with our advances in technology, provides us with the balance best suited in finding the right solutions.

Multifield Mapping

Large area mapping in EDS:

X-ray maps in EDS are most often collected using only beam deflection in a single field of view. Using this method, a beam rasters over an area defined by the pixel resolution of the matrix. The time spent by the beam on each pixel is set by the dwell time.

EDS maps can either be region-of-interest (ROI), count, or full quantification. Using spectral mapping, an EDS spectrum is stored in each pixel to allow post processing on the raw data. For larger area maps, beam deflection is used in combination with movements of the SEM stage to perform Multifield Mapping.

With the use of silicon drift detectors (SDD), capable of handling very high count rates without significant loss of resolution, good quality large area mapping can be done in a very short time.

The first step in Genesis is the set up. Single points can be defined and put into a stage table. Each time the stage is at a new location, the "First" button should be pressed to update the new stage values and then added to the Table. When using line or matrix, the starting stage position is chosen and the "First" button is pressed. After moving to the end point the "Last" button is pressed. When number of points (line) or matrix size has been defined, it can be added to the stage list.

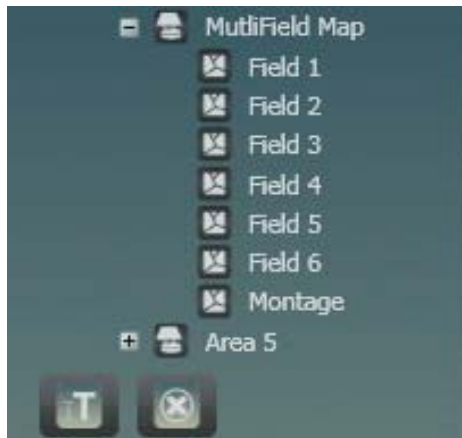


Figure 1. Multifield Map files in TEAM™ EDS.

The adjacent field option can be selected in conjunction with locking the current magnification or the specified number of fields. A pop-up will be generated that offers a suggested change in the number of fields or magnification respectively. The

recommended changes ensure that no overlapping of the fields, or unanalyzed spacing, is introduced to the specified analysis area. After the data collection is completed, stitching of the fields could then be done using spectrum utilities.

In TEAM™ EDS software, the stitched images and X-ray maps (montage) are automatically created when the Multifield analysis has finished (see figure 1).

Figure 2 shows a 4x5 matrix Multifield Mapping of a geological sample. It was recorded at 25kV using an Apollo XP SDD at 50kcps count rate; resolution at MnK α =125 eV. It took a little more than one hour to record this large area EDS map.

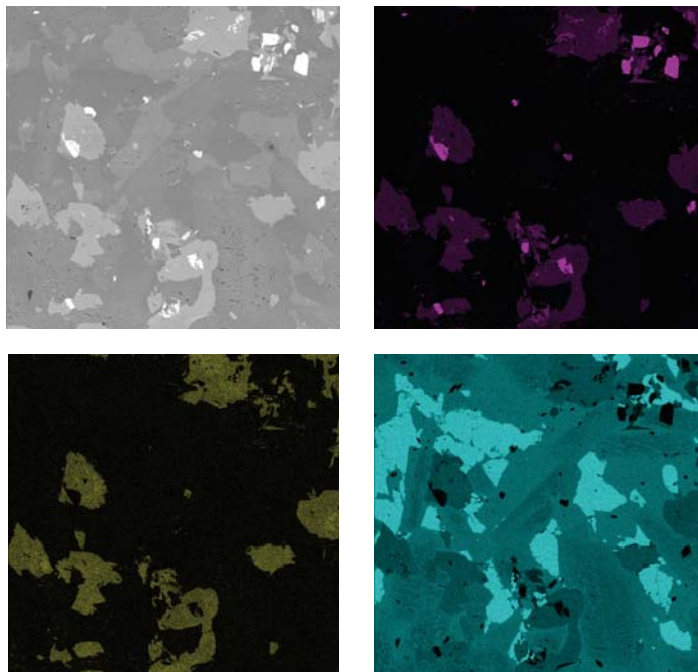


Figure 2. Multifield Maps (upper left=BSE image, upper right=FeKa map, lower left=MgKa map, lower right=SiKa map).

EBSD Characterization of Stress Corrosion Cracks in 2124 Aluminum Alloys

Stress corrosion cracking is a fracture mode that is caused by the combined effects of stress and a chemical attack. Stress corrosion cracking can occur without any external loads. Therefore, stress corrosion can cause detrimental failure without any obvious degradation on the surface of the component.

The 2xxx series aluminum alloy is one of the highest strength aluminum alloys. Even though the 2xxx series is widely used in structural materials that require high strength-to-weight ratios, such as truck and aircraft wheels, truck suspension parts, and aircraft fuselages, it is nevertheless susceptible to stress corrosion cracking. The aluminum alloy 2124 used in this study has a nominal chemical composition (wt %) of Cu: 3.8, Mg: 1.2, Mn: 0.48, Fe: 0.09, Si: 0.04, Zn: 0.04, Ti: 0.02, and balance Al.

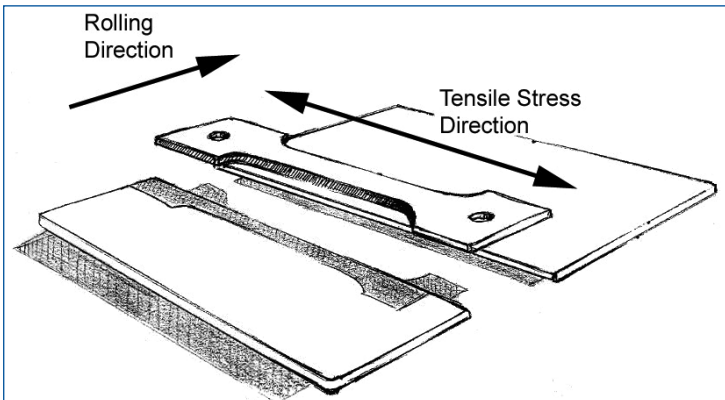


Figure 1 – Diagram showing the orientation of the dog-bone sample and the direction of the tensile sample axis, cut from the rolled aluminum alloy.

The 6.3mm thick samples first underwent a heat treatment of 350°C for 120 minutes followed by air cooling before it was subsequently cold rolled to 82% reduction in thickness. After cold working, the samples received a solutionizing heat treatment of 500°C for 30 minutes. The samples were then quenched in room temperature water before being subjected to an aging treatment of 160°C for 16 hours. Following heat treatment, tensile “dog-bone” shaped samples were cut from the plates with the tensile sample axis oriented parallel to the rolling direction as shown in Figure 1. A static tensile stress of 29ksi was then applied to the tensile specimens by mounting the samples in a bracket that holds the sample in place. The stressed samples were then submitted to an alternate immersion test, whereby the samples were cycled between soaking in a 3.5%NaCl solution for 10 minutes, and drying in air for 50 minutes.

Cross-sections perpendicular to the rolling plane were mechanically polished for microstructural characterization through Orientation Image Mapping (OIM™). Electron Backscatter Diffraction (EBSD) data was collected with an accelerating voltage of 20kV, a working distance of approximately 17mm, and a step size of 1μm scanning on a hexagonal sampling grid. An inverse pole figure map collected around a stress corrosion crack is shown in Figure 2. The stress corrosion crack is clearly visible as black points in Figure 2 since no diffraction data could be obtained from those points.



Figure 2 – An inverse pole figure map showing the EBSD data obtained from OIM around a stress corrosion crack found in the corroded 2124 aluminum alloy.

Figure 3 demonstrates a new feature in OIM™ version 6.0, where users can visualize pole figures and orientation distributions in three-dimensions. The {001} pole figure and the orientation distribution plot measured from the corroded samples show that the material has the expected recrystallization texture of face-centered cubic (FCC) materials or cube texture. The orientation distribution plot displays the crystal orientations in their respective Euler angles. Because aluminum is FCC and has cubic symmetry, the three Euler angles only range from 0-90°.

(Cont'd on Pg. 5)

EBSD Characterization of Stress Corrosion Cracks in 2124 Aluminum Alloys (Cont'd. from Pg. 4)

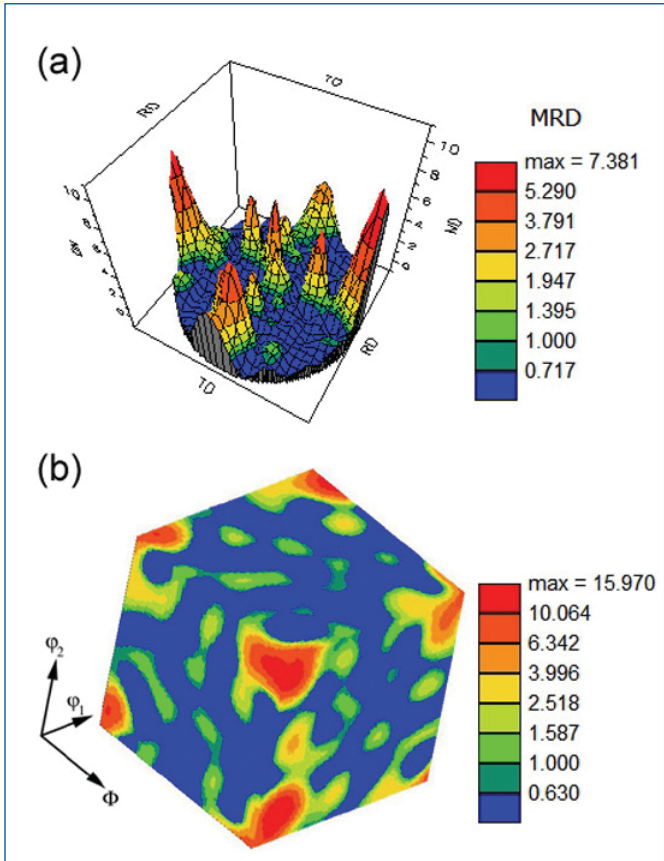


Figure 3 – (a) A three-dimensional {001} pole figure, and (b) orientation distribution plot in Euler angle space. Both figures were generated with OIM™ version 6.0 and show that cube texture was observed in the heat treated 2124 aluminum alloy.

The number fraction of boundaries with different misorientation angles is plotted in Figure 4. The misorientation angle plot shows the distribution of boundaries for the EBSD data portrayed in Figure 2 as well as a subset of misorientations that were measured across the crack. As seen in Figure 4, the heat-treated aluminum alloy contains a higher than random fraction of low angle grain boundaries ($\Delta\theta \leq 15^\circ$) as compared to the random (McKenzie) distribution. When comparing the cracked boundaries to all the boundaries observed in the sample, the low angle grain boundaries appear to have a higher resistance to stress corrosion cracking than high angle grain boundaries.

Grain boundary dependent properties, such as fracture and intergranular corrosion, are strongly dependent on the crystallographic nature of the grain boundaries. The concept of “Grain Boundary Design and Control”, otherwise known as “Grain Boundary Engineering” (GBE), was first introduced by Watanabe in 1984. GBE asserts that by manipulating the grain boundary character distribution to generate a higher fraction of low-energy Coincident Site Lattice (CSL) boundaries, the crack or corrosion resistance of the material can be improved. GBE studies on nickel-based alloys and austenitic stainless steels have shown that the corrosion resistance of the material increased with an increasing fraction of low CSL boundaries ($\Sigma \leq 29$). GBE may be applied to the current study of the 2124 aluminum alloy to increase the distribution of CSL boundaries which may in turn increase the stress corrosion resistance of the material.

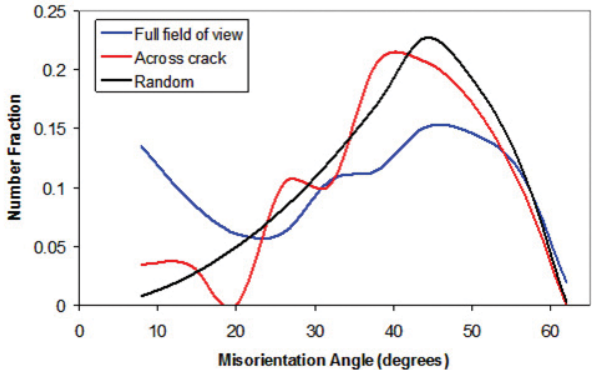


Figure 4 – Number fraction plotted as a function of grain boundary misorientation angle. The blue line corresponds to the boundary misorientations that are observed from the full field of view in Figure 2, while the red line corresponds to the boundary misorientations that are measured across the crack.

World-Wide Events

EDAX is pleased to announce that we are now on Facebook and LinkedIn. View our page for new product information, software updates, training, News & Events, and much more. If you not have not already done so, join Facebook and LinkedIn to get the latest up-to-date EDAX information.

<http://www.facebook.com/home.php?#/pages/Mahwah-NJ/EDAX/157350931061>

http://www.linkedin.com/company/edax?goback=%2Ecps_1288809548767_1&trk=co_search_results

2011 Schedule

March 13-18	Pittcon	Atlanta, GA
May 16-18	Japanese Society of Microscopy 2011	Fukuoka, Japan
August 7-11	M&M (Microscopy & Microanalysis)	Nashville, TN
September 7-9	JAIMA	Chiba, Japan

***Please see our website www.edax.com for a complete list of our tradeshow

World-Wide Training

To help our present and potential customers obtain the most from their equipment and to increase their expertise in EDS microanalysis, WDS microanalysis, EBSD/OIM™ and Micro-XRF, we organize a number of Operator Courses at the EDAX facilities in North America; Tilburg, NL; Wiesbaden, Germany; and Japan.

Europe

Tilburg = (T) (in English)

Wiesbaden = (W) (in German unless stated otherwise):

EDS Microanalysis: (Genesis)

- ◆ February 15-17 (T)
- ◆ May 10-12 (T)
- ◆ June 28-30 (T)
- ◆ November 22-24 (T)

EDS Microanalysis: (TEAM)

- ◆ March 29-31 (T)
- ◆ May 23-25 (W)
- ◆ September 27-29 (T)
- ◆ Nov. 1-Dec. 29 (W)

EDS Microanalysis: (Short)

- ◆ March 17-18 (T)
- ◆ June 23-24 (T)
- ◆ September 27-29 (T)
- ◆ November 10-11 (T)

EBSD:

- ◆ March 14-16 (T)
- ◆ June 20-22 (T)
- ◆ September 19-21 (T)
- ◆ November 7-9 (T)

WDX TEXTS:

- ◆ May 25-26 (W)

WDS LEXS:

- ◆ April 12-14 (T)
- ◆ October 11-13 (T)

Orbis:

- ◆ May 9-11 (W)
- ◆ October 26-28 (W)

Pegasus (TEAM/EBSD):

- ◆ March 21-25 (W)
- ◆ October 17-21 (W)

Japan

Microanalysis Courses:

- ◆ February 23-25 Tokyo
- ◆ April 13-15 Osaka
- ◆ June 8-10 Tokyo
- ◆ July 6-8 Osaka
- ◆ October 5-7 Tokyo
- ◆ November 9-11 Osaka

For more information on our training classes, please visit our website at:

www.edax.com/service/user.cfm

North America

EDS Microanalysis:

- ◆ March 8-10 Mahwah, NJ
- ◆ May 2-6 Mahwah, NJ
- ◆ June 21-23 Mahwah, NJ
- ◆ July 12-14 Draper, UT
- ◆ September 13-15 Mahwah, NJ
- ◆ October 10-14 Mahwah, NJ
- ◆ November 8-10 Mahwah, NJ

EBSD :

- ◆ May 10-12 Mahwah, NJ
- ◆ August 20 - Sept. 1 Mahwah, NJ
- ◆ September 27-29 Draper, UT

Pegasus :

- ◆ February 7-11 Draper, UT

EDS Particle Analysis:

- ◆ April 12-14 Mahwah, NJ

WDS:

- ◆ June 7-9 Mahwah, NJ

Micro-XRF:

- ◆ March 29-31 Mahwah, NJ
- ◆ October 4-6 Mahwah, NJ



Weimin Xia joined EDAX in February 2001 as an Application Specialist based in the China office located in Beijing. He graduated from Tsinghua University with a Bachelor of Engineering degree and a specialty in Metal Material.

Weimin has an impressive scientific background. He held the position of Assistant Research Professor (Lecturer) and Chief of SEM Laboratory at the State Laboratory of Tribology, Tsinghua University. Among other things, Weimin taught a course in microanalysis of metals. He also worked as an Assistant Engineer at The Electric Power Construction Research Institute under the Chinese Ministry of Energy Resource. While in that position Weimin was an EDAX EDS user. He also held the position of Product Specialist for Carl Zeiss China.

Weimin has worked for EDAX for the past nine years and is responsible for the EDS, WDS, and Micro-EDXRF product lines. His product knowledge and expertise are used throughout China to support EDAX customers. He also assists with translation of the EDAX software and marketing material to the Mandarin language.

In his spare time, Weimin enjoys spending time with his wife Song Yun. They enjoy hiking in the mountains. He also enjoys listening to classical music, playing the clarinet as well as reading modern technology publications.



Craig Theberge joined EDAX in April 2001 as the USA Southeastern Field Service Engineer. Craig is located at the edge of the Smoky Mountains in Chattanooga, TN. Prior to joining EDAX he worked with Tracor Northern from 1989-1996 as a Field Service Engineer, and Evex from 1996-2001 as a Sales and Service Consultant.

Craig began his career as a Paratrooper in the U.S. Army where he earned the rank of Sergeant. He served as an Artillery Fire Direction Section Chief in the 82nd Airborne Division. After his military service, Craig earned an Associates Degree in Electronics from Devry Institute of Technology, and began his tenure with Tracor. Craig went back to school after his children were grown and earned a Bachelor of Science Degree in Technical Management from Devry University in 2007.

Craig moved into his current role as the Southeast Sales Manager in 2007. Craig is responsible for instrument sales in the Southeast region. Among his many tasks are interfacing with the various electron microscope sales representatives, coordination between applications and service departments during system evaluation and commissioning, and most importantly, ensuring customer satisfaction in his territory.

In his spare time Craig enjoys working on projects around his home and spending time with his wife Barbara, their children, and grandchildren. Craig also volunteers his time in the community and church.

Alcoa Howmet Research Center (AHRC), Whitehall, MI

Alcoa Howmet Research Center (AHRC) in Whitehall, MI provides support to Alcoa Howmet facilities including super alloy investment foundries, titanium and super alloy manufacturing facilities, and ceramic manufacturing plants. In addition to internal support, AHRC also performs as an independent laboratory, providing testing for a wide industrial base, including automotive, glass, and electrical component manufacturers.

AHRC is a full service characterization lab, with chemical composition analysis, metallography, mechanical testing, heat treat and instrumentation calibration capabilities. The work performed in the AHRC is a key component of manufacturing cost savings initiatives for Alcoa Howmet plants.



Photo courtesy of Alcoa-Howmet

In early 2009, AHRC expanded its microanalytical capabilities with the addition of an EDAX Trident system, installed on a JEOL 6610LV microscope. Beyond its use in root cause analysis, the integrated EDS, EBSD and WDS system supports research and development and failure analysis initiatives. At the AHRC, EDS

detection is performed with the Apollo 40 silicon drift detector system. Eliminating the use of liquid nitrogen and increasing analytical throughput has provided the AHRC with a time saving benefit. The LEXS WDS spectrometer was acquired as a confirmatory or back-up tool for a Cameca microprobe, which is used primarily for quantifying aerospace coating composition, and will be used simultaneously with the EDS to resolve difficult-to-discern peak overlaps or to analyze elements in low levels that are beyond EDS capability.

Traditionally, grain size analysis was performed with optical microscopy per ASTM E112. AHRC supplements this testing with the use of the DigiView IV EBSD camera and OIM™ software suite. EBSD can provide an advantage where grain boundaries are difficult to discern by optical microscopy. In addition to grain size analysis, AHRC is also using EBSD to characterize grain orientation of various samples.

Personnel from AHRC have attended EDAX training in all three disciplines at the facilities in Draper, UT and Mahwah, NJ, and continue to work with EDAX staff in applications development. "I never hesitate to call EDAX personnel for help and they are responsive and understand my applications. The training provided by EDAX has been essential to minimizing the amount of time it took to learn the EDAX software, hardware and terminology", says Jim Way, AHRC Microanalysis Team Leader. The EDAX Trident is an integral part of the AHRC's suite of analytical tools, and will serve as a base for much future development.

Art & Layout:

Beverlee Boddy
Christine Meehan

Contributing Writers:

Lisa Chan
Laurie Carlone
Sun Park
Alan Sandborg
Craig Theberge
Harry Verhulst
Weimin Xia



Copyright 2010 EDAX Inc. No part of this publication may be reproduced, stored in a retrieval system, or transmitted in any form or by any means without prior written permission of EDAX Inc.



EDAX Inc. • 91 McKee Drive Mahwah, NJ 07430 • Phone: (201) 529-4880 • E-mail: info.edax@ametech.com • www.edax.com